Nucleic Acids Research, 2006, Vol. 34, No. 6 ***e48***
doi:10.1093/nar/gkl055

Fast Fenton footprinting: a laboratory-based method for the time-resolved analysis of DNA, RNA and proteins

Inna Shcherbakova, Somdeb Mitra, Robert H. Beer[1] and Michael Brenowitz*

Department of Biochemistry, Albert Einstein College of Medicine, 1300 Morris Park Avenue, Bronx, NY 10461, USA and [1]Department of Chemistry, Fordham University, 441 East Fordham Road, Bronx, NY 10458, USA

Received January 13, 2006; Revised February 14, 2006; Accepted February 24, 2006

ABSTRACT

'Footprinting' describes assays in which ligand binding or structure formation protects polymers such as nucleic acids and proteins from either cleavage or modification; footprinting allows the accessibility of individual residues to be mapped in solution. Equilibrium and time-dependent footprinting links site-specific structural information with thermodynamic and kinetic transitions. The hydroxyl radical (·OH) is a particularly valuable footprinting probe by virtue of it being among the most reactive of chemical oxidants; it reports the solvent accessibility of reactive sites on macromolecules with as fine as a single residue resolution. A novel method of millisecond time-resolved ·OH footprinting has been developed based on the Fenton reaction, $Fe(II) + H_2O_2 \rightarrow Fe(III) + {\cdot}OH + OH^-$. This method can be implemented in laboratories using widely available three-syringe quench flow mixers and inexpensive reagents to study local changes in the solvent accessibility of DNA, RNA and proteins associated with their biological function.

INTRODUCTION

'Footprinting' describes assays in which ligand binding or structure protects polymers such as nucleic acids and proteins from either cleavage or modification; footprinting allows the accessibility of individual residues to be mapped in solution. Equilibrium and time-dependent footprinting links site-specific structural information with thermodynamic and kinetic transitions (1,2). The hydroxyl radical (·OH) has proven itself as a particularly valuable footprinting reagent by virtue of it being among the most reactive of chemical oxidants (3). Its small radius reports the solvent accessibility of reactive sites on macromolecules with resolution as fine as a single residue (4,5). Multiple methods have been used to ·OH footprint DNA, RNA and proteins including Fe-EDTA (6,7), peroxonitrite (8–10), photolysis (11–13), radiolysis (14–16) and synchrotron X-ray radiolysis (17). Fe-EDTA footprinting uses the Fenton–Haber–Weiss reaction (18,19),

$$Fe(II) + H_2O_2 \rightarrow Fe(III) + {\cdot}OH + OH^- \qquad \mathbf{1}$$

to generate ·OH in solution (20). Chelation of Fe(II) by EDTA prevents the transition metal ion from binding to the macromolecules being studied (20). This method is widely applied and inexpensive to perform. A convenient implementation of this chemistry for footprinting is to reductively cycle Fe(III) back to Fe(II) with ascorbate (21). This catalysis allows reagent concentrations that are micromolar in Fe-EDTA and millimolar in H_2O_2 and ascorbate to be used with reaction times of several to tens of minutes (4,6,22). Reaction times as short as several seconds in an RNA folding kinetics analysis were achieved using a Fe-EDTA concentration of 500 μM (23).

Exhaustive investigations of the Fenton reaction have revealed numerous possible reaction steps, variable rates, mechanisms, intermediates and putative oxidants depending on which reagents and reaction conditions are used [(24) and references therein]. However, limited studies of the Fenton reaction (25) have been carried out at Fe(II) concentrations >1 mM. It is possible that such high Fe(II) concentrations might produce the high concentration of ·OH needed to footprint macromolecules on the millisecond timescale (23). Rapid mixing studies at high Fe(II) concentrations have not been reported to our knowledge.

Synchrotron X-ray radiolysis has been unique among available ·OH footprinting methods in that a millisecond burst of high-flux white X-ray generates ·OH sufficient to footprint nucleic acids (17). Macromolecular transitions can be followed with millisecond time resolution by coupling rapid mixing with synchrotron X-ray radiolysis (2,26,27).

*To whom correspondence should be addressed. Tel: 00 1 718 430 3179; Fax: 00 1 718 430 8565; Email: brenowit@aecom.yu.edu

Widespread application of 'synchrotron footprinting' has been limited by the scant availability of suitable beamlines and the need for investigators to travel to a remote facility. The fast Fenton footprinting method presented in this paper allows time-resolved ·OH footprinting to be conducted within laboratories using widely available three-syringe quench-flow mixers. Cation-mediated RNA folding results are presented to validate the method and demonstrate the novel information that can be obtained by its use; the applicability of fast Fenton footprinting to proteins is discussed.

MATERIALS AND METHODS

Reagents

A 0.4–0.5 mM fluorescein (Molecular Probes) stock solution was prepared in 10 mM Tris–HCl, pH 7.6, and 10% glycerol and stored at −20°C. This solution was diluted to 20 nM in assay buffer prior to stopped-flow measurements. L-21 ScaI ribozyme from *Tetrahymena thermophila* was 5′ end radiolabeled with [γ-^{32}P]ATP (28). A HindIII/NdeI DNA restriction fragment of 282 bp from plasmid ppUMLP was ^{32}P-labeled at the HindIII site and gel purified (29,30). The radiolabeled nucleic acids were stored in 10 mM sodium cacodylate, pH 7.3, at −70°C.

A stock solution of 100 mM $Fe(NH_4)_2(SO_4)_2$ (Sigma-Aldrich) was prepared and stored in small aliquots at −70°C. Stock solutions of 500 mM Na_2-EDTA (Ambion) and 30% H_2O_2 (Fluka) were kept at room temperature and +4°C, correspondingly. The 10× 'assay buffer' (200 mM sodium cacodylate, 2 M NaCl at pH 7.4) and standard quench solution (50 mM thiourea, 20 mM EDTA and 200 mM NaCl) were prepared and stored at +4°C. An 'alternative quench solution' is absolute ethanol that facilitates subsequent precipitation of nucleic acids. The presence of ·OH scavengers (e.g. Tris and HEPES buffers, DTT and glycerol) (21) requires either higher concentrations of Fe(II)-EDTA and H_2O_2 and/or longer reaction times.

Stopped-flow dye degradation assay of ·OH production

A simple assay for ·OH production was developed that follows the quenching of the fluorescence emission of fluorescein upon dye oxidation (31,32). Fluorescein was used due to its high quantum efficiency, solubility and ready availability. In these experiments, a solution of H_2O_2 and dye were mixed with Fe(II)-EDTA and the fluorescence emission at 520 nm, following 490 nm excitation, monitored (Figure 1A). Experiments were conducted in 'assay buffer' containing 20 mM sodium cacodylate and 200 mM NaCl at pH 7.4 and 25°C. To follow Fe(II) to Fe(III) conversion fast changes in absorption at 350 nm were monitored upon mixing of 2 mM of Fe(II)-EDTA solution and 0.3% H_2O_2 (33). The stopped-flow experiments were conducted using an Applied Photophysics PiStar-180 mixer with fluorescence and absorption optics.

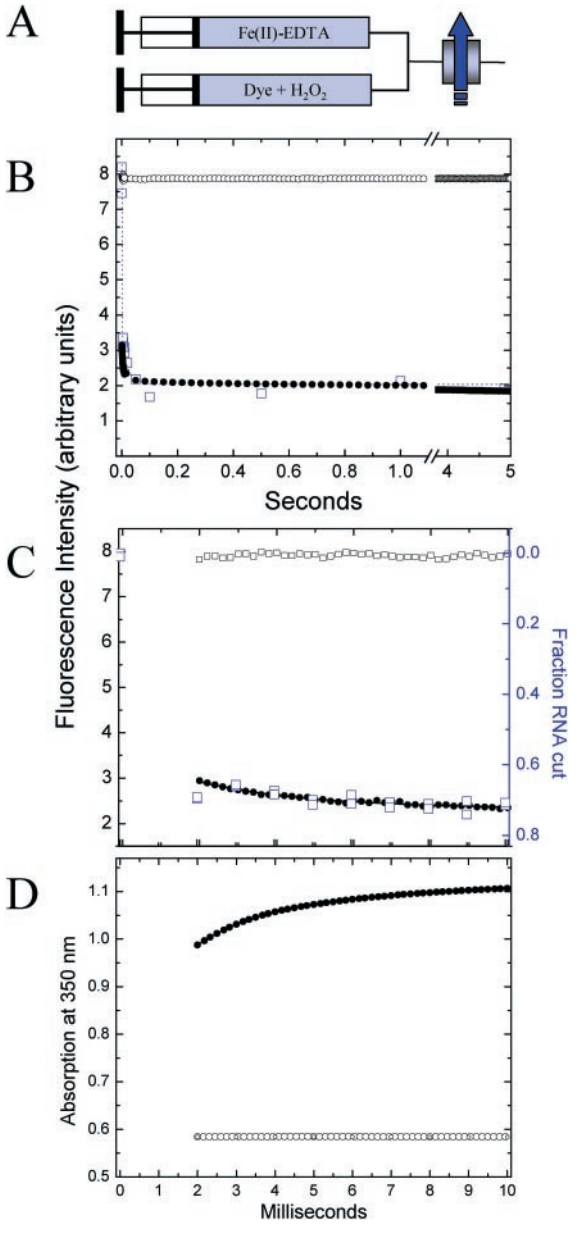

Figure 1. (**A**) Schematic representation of the stopped-flow mixing experiments. The arrow indicates fluorescence detection; (**B** and **C**) Quantification of ·OH production by loss of fluorescence emission of fluorescein following the mixing equal volumes of solutions containing Fe(II)-EDTA and H_2O_2 in assay buffer at 25°C to final concentrations of 10 and 133 mM (0.45%), respectively. (C) is an expansion of the first 10 ms of (B). The closed symbols track the oxidation of fluorescein. The open symbols depict the control in which the fluorescein and H_2O_2 were mixed with buffer. Five 'shots' were averaged. Every second and fourth data point is displayed in (C) and (D) for clarity. The blue open squares in (B) depict the fluorescein oxidation experiment conducted in the quench-flow mixer. The blue open square symbols in (C) depict the cleavage of ^{32}P-RNA in the quench-flow mixer. The solid line depicts the best fit of an exponential decay to the stopped-flow fluorescence data over the 10 ms duration shown in (C) with $y_0 = 2.326 \pm 0.007$; $A = 1.143 \pm 0.028$ and $t = 3.0 \pm 0.1$ ms; (**D**) Direct measurement of the oxidation of 1 mM Fe(II) to Fe(III) by 44 mM H_2O_2 by following the absorption increase at 350 nm (33). The 350 nm wavelength is on the shoulder of the iron-chelator absorption spectrum separate from H_2O_2 absorption. The data are best fit to a bi-exponential decay with $y_0 = 1.129 \pm 0.002$; A_1, $t_1 = -0.265 \pm 0.002$, 1.45 ± 0.01 ms; A_2, $t_2 = -0.101 \pm 0.002$, 6.57 ± 0.04 ms. Reactions involving Fe(II), Fe(III) and H_2O_2 and their products in addition to reaction 1 have been documented at the reagent concentrations being used in this footprinting protocol (25) and are the likely source of observed multiple kinetics phases. These additional reactions are not considered herein since the slower kinetic phases do not significantly contribute to the footprinting reaction.

DNA or RNA dose–response

Dose–response experiments were conducted, as follows, using a KinTek® RQF-3 three-syringe mixer following the 'quench-flow run' control option (27,34,35):

i. Load the drive syringes with 1× assay buffer and the quench syringe with the standard quench solution or ethanol (Figure 3A).
ii. Prepare the following solutions:
   a. ^{32}P-DNA or ^{32}P-RNA (~100 000 d.p.m./data point) solution in 1× assay buffer containing H_2O_2 to the desired concentration. The final volume prepared depends on the number of data points to be collected (20 µl per point). H_2O_2 containing solutions should be protected from light to minimize ·OH production by photolysis (11).
   b. The same volume of $Fe(NH_4)_2(SO_4)_2$ to the required concentration and EDTA to 1.1 times the Fe(II) concentration in 1× assay buffer.
iii. Inject several nucleic acids samples against 1× buffer to acquire several zero time point measurements.
iv. Inject nucleic acids samples against the Fe(II)-EDTA solution, incrementing the delay time to acquire the desired range of aging times. The mixer should be cleaned and primed between each data point following the manufacturer's protocol. Each expelled solution is separately collected and stored on ice until the completion of the time course.
v. Separate the ·OH cleavage products by denaturing gel electrophoresis and visualize them by a storage phosphor screen (17,27). The fraction of nucleic acid cleaved is calculated from the ratio of the density of the cleaved molecules to the total.

General protocol for fast Fenton footprinting

Fast Fenton footprinting required only minor alteration of the standard control protocol for the three-syringe quench-flow mixer. Our protocol for the KinTek® stepper motor, equipped with a RCF-3 mixer, is compatible with other devices. Selecting the 'Constant quench volume' option from the 'Alter quench parameters' menu of the KinTek® control program keeps the delivered volume constant during acquisition of a dataset. The 5 ms ·OH production time used in the present protocol was achieved by shortening the mixer's exit tube and increasing the minimum motor speed to 430 r.p.m. (see Appendix).

The KinTek® mixer ages binding or folding reactions in one of two ways. Longer aging time (a 'pause') is achieved by stopping and restarting the motor. Shorter aging times are achieved by using shorter reaction loops while keeping the motor running at a constant, albeit different, speeds. For this reason the ·OH production time varies from 3 to 6 ms for aging times <36 ms. However, this variation did not result in detectable differences in nucleic acid cleavage due to the large burst amplitude in the ·OH production kinetics (Figure 4A); most ·OH production occurs during the first millisecond after mixing with Fe(II)-EDTA.

Below are the steps for conducting a footprinting experiment to detect folding or ligand binding of nucleic acids:

i. Load the two drive syringes with 1× assay buffer and the quench syringe with the appropriate concentration of freshly prepared Fe(II)-EDTA in 1× assay buffer.
ii. Prepare the following solutions:
   a. ^{32}P-DNA or ^{32}P-RNA (~600 000 d.p.m./data point) (Figure 5A, Reactant 'A') in 1× assay buffer. The final volume prepared depends on the number of data points to be collected (20 µl per point). A little excess allows for mistakes and data point additions.
   b. Same volume of a solution of reactant 'B' (twice the desired final concentration) and H_2O_2 (triple the final concentration) in 1× assay buffer (Figure 5A).
   c. H_2O_2 solution (triple the desired final concentration) in 1× assay buffer. Volume should be enough for acquisition of several zero time point measurements.
   d. Fresh 5 ml of Fe(II)-EDTA solution (triple the desired final concentration) in 1× assay buffer. Reactant 'B' can optionally be included at its final desired concentration to prevent its dilution upon mixing the aged reactants with this solution.
   e. Equal volume of standard quench solution or three volumes of ethanol (relative to the volume expelled by the mixer) in a set of collection tubes.
iii. To document the integrity of the input nucleic acid, inject nucleic acids samples with 1× assay buffer and expel into the collection tubes containing the quench solution. Perform replicates. Clean and prime the mixer between each data point collection following the manufacturer's protocol.
iv. For zero time point measurements inject nucleic acids samples with 1× assay buffer containing only H_2O_2 and expel into the collection tubes containing the quench solution.
v. For time points of transition, inject the nucleic acid solution against the solution containing reactant 'B' and H_2O_2, incrementing the delay time until the desired range of aging times is acquired. Collect each expelled solution separately and store on ice until the time course is complete.
vi. Separate the ·OH cleavage products by denaturing gel electrophoresis and visualize by a storage phosphor screen (17,27).

Data analysis

The digital autoradiograms are quantified using either a 'box analysis' (36) or single band peak fitting using the program SAFA (37). The time-dependent changes in band intensities are transformed into an ensemble of structurally localized kinetics progress curves which can be analyzed to yield kinetic models of the process (26,38,39).

Application of fast Fenton footprinting to RNA folding

Folding of the *Tetrahymena* ribozyme at 42°C was initiated with 10 mM $MgCl_2$ in either a low salt buffer containing 10 mM sodium cacodylate and 0.1 mM EDTA (pH 7.3) or a high salt buffer containing an additional 200 mM NaCl. A solution containing $MgCl_2$ and H_2O_2 in buffer was mixed against the ^{32}P-RNA (Figure 5A) and the reaction was aged for a defined time. The Fe(II)-EDTA solution was

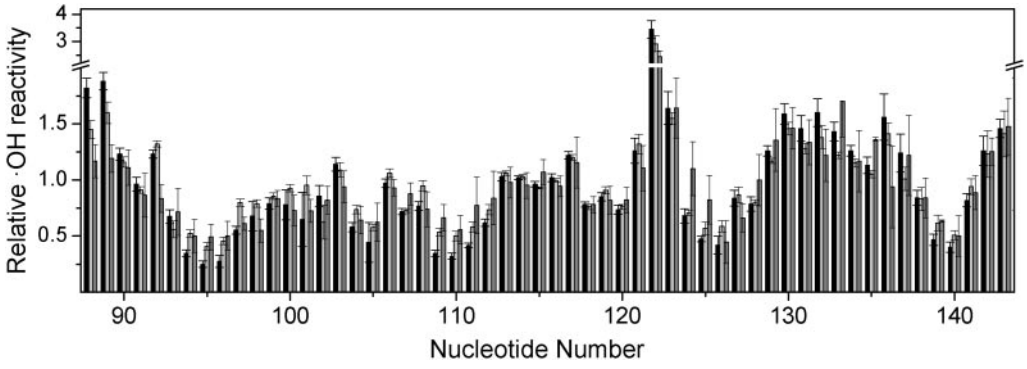

Figure 2. Quantification (37) of the ·OH reactivity profile of the Mg^{2+}-folded *Tetrahymena* ribozyme nt 88–143 obtained by fast Fenton (black bars), Fenton/Ascorbate (light grey bars) and synchrotron X-ray (dark grey bars) footprinting. The Fenton/Ascorbate reaction and X-ray radiolysis were conducted as described in the literature (22,35).

then added from the 'quench syringe' to initiate ·OH production and RNA cleavage for a suitable time period, as determined previously from the dose–response experiments, to achieve single hit kinetics. Expelling the sample into a collection tube containing the quench solution stops the reaction (Figures 1–3).

RESULTS

Fast ·OH generation from Fe(II)-EDTA and H_2O_2

The production of ·OH was assayed by the decrease in fluorescein dye fluorescence resulting from its oxidation following stopped-flow mixing of Fe(II)-EDTA and H_2O_2 as illustrated in Figure 1A (31). Detectable degradation of the dye is not observed upon incubation with only H_2O_2 (Figure 1B, open circle). In contrast, ~75% of the dye fluorescence is lost within seconds when Fe(II)-EDTA and H_2O_2 are mixed together to final concentrations of 10 and 130 mM (0.45%), respectively (Figure 1B, closed circle). This reaction does not require ascorbate. Inspection of the first 10 ms of the reaction reveals that ~40% of the dye fluorescence is lost within the 2 ms mixing dead time with only ~10% further decay over the next 8 ms (Figure 1C, closed circle). These results show that ·OH is quickly and liberally generated from mM concentrations of Fe(II)-EDTA and H_2O_2.

The increase in metal absorption at 350 nm over the same timescale (Figure 1D, closed circle) shows that Fe(II) is oxidized to Fe(III) during this transition (33). Conversely, ·OH is not generated when Fe(III)-EDTA is substituted for Fe(II)-EDTA (data not shown). These results are consistent with the production of ·OH by reaction 1. We next asked whether ·OH is the oxidant in the footprinting reactions (20). The correspondence between ·OH reactivity patterns for nucleic acids in solution with the solvent accessible surface of the phosphodiester backbone calculated from crystal structures has been established for radiolytic and Fenton/Ascorbate footprinting (22,39,40). That this relationship holds true for fast Fenton footprinting is shown in Figure 2; identical footprinting profiles are observed for a Mg^{2+}-folded RNA regardless of whether ·OH is generated by synchrotron radiolysis of water (in 15 ms), Fe(II)-EDTA/H_2O_2/ascorbate (in 2 min) or Fe(II)-EDTA/H_2O_2 (in 5 ms). We conclude from these results that ·OH is the common reactive species.

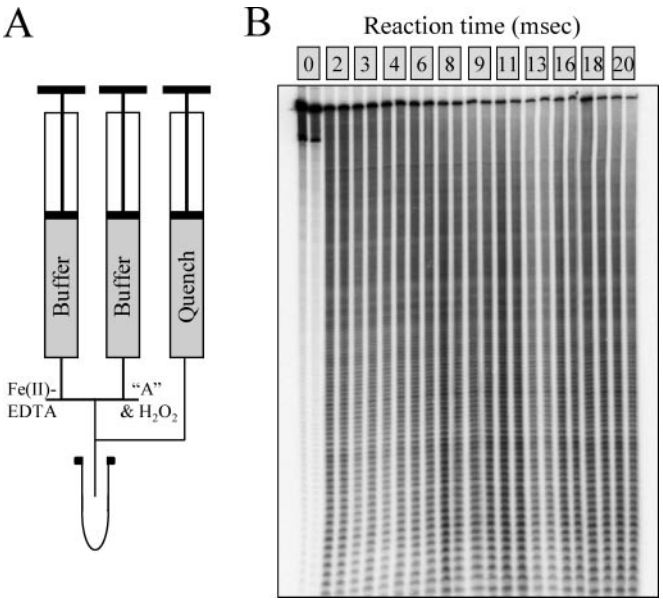

Figure 3. (**A**) Schematic representation of the dose–response experiment conducted in the quench-flow mixer. 'A' denotes the molecule being analyzed, in this case a 282 bp ^{32}P end-labeled DNA restriction fragment. (**B**) Autoradiogram of the cleavage products produced following mixing of Fe(II)-EDTA and H_2O_2 to final concentrations of 5 and 44 mM (0.15%), respectively, to produce ·OH for the indicated number of milliseconds.

Rapid termination of ·OH production

Since stopped-flow mixing experiments follow ·OH production in real time, the rapidity with which this reaction is terminated does not influence these measurements. In contrast, fast quenching of ·OH mediated oxidation is as important as fast radical production for the development of a quench-flow footprinting protocol. The footprinting reaction will continue past the desired interval unless the iron present in solution is inactivated or the additional ·OH that is produced is scavenged. Therefore, we assessed whether the ·OH footprinting reaction is terminated in the quench-flow mixer by the addition of an excess of scavenger by comparing dye degradation progress curves obtained by stopped- and quench-flow mixing

(Figure 3A, where 'A' is dye). A series of time-points were collected and the fluorescence of each data point analyzed. The stopped- and quench-flow decay curves are coincident (Figure 1B; compare closed circle with open square) demonstrating that an excess of ·OH scavenger effectively ends the footprinting reaction.

Footprinting DNA and RNA

When the quench-flow mixing experiment shown in Figure 3A is conducted with 'A' as RNA, RNA cleavage is comparable to that of the dye degradation at identical concentrations of Fe(II)-EDTA and H_2O_2 (Figure 1C; compare closed circle with open square). Approximately 75% of the RNA molecules are cleaved at least once within 2 ms; this amount of oxidative cleavage exceeds the 'single-hit' kinetics desired for quantitative footprinting (36). Thus, the moderate concentrations of Fe(II)-EDTA and H_2O_2 used in these experiments produces more than enough ·OH for nucleic acid footprinting with millisecond time resolution.

Figures 3B and 4 show 'dose–response' relationships for DNA and RNA obtained at identical concentrations of Fe(II)-EDTA and H_2O_2 that relate ·OH production to nucleic acid cleavage. Three aspects of the autoradiogram shown in Figure 3B should be noted: (i) appreciable DNA cleavage occurs within the earliest sampling of 2 ms with the intensity of the full-length DNA band at the top of the gel decreasing with increasing reaction time; (ii) the distribution of ·OH reaction products is uniform at the short reaction times as expected for single-hit cleavage; (iii) the distribution of reaction products is increasingly biased towards small fragments at long reaction times due to multiple cutting as predicted by Poisson statistics (36).

Quantification of DNA or RNA cleavage yields the dose–response curves upon which footprinting protocols are based (Figure 1C, open square, and Figure 4A). Like the dye degradation data, the DNA and RNA dose–response curves display large burst amplitudes at these reagent concentrations; the observable portion of the nucleic acid curves is adequately fit to a single exponential. While both DNA and RNA are rapidly and efficiently cleaved, DNA degradation is more efficient compared with RNA consistent with the latter nucleic acid's oxidative stability (41). The increase in nucleic acid cleavage with increasing [Fe(II)-EDTA] at constant [H_2O_2] and reaction time is expected for a bimolecular reaction (Figure 4B). These results show that as little as 1 mM Fe(II)-EDTA and 44 mM H_2O_2 is sufficient for millisecond nucleic acids footprinting.

A protocol was devised that allows time-resolved footprinting of macromolecular transitions to be followed with millisecond time resolution using a three-syringe quench flow mixer (Figure 5A). Key to this method are the minimal ·OH generated from H_2O_2 in the absence of Fe(II) and the rapid termination of the ·OH footprinting reaction when a sample is expelled into a quench solution. The method also relies upon a constant duration between addition of the Fe(II)-EDTA solution and quenching. The large burst amplitude for ·OH production makes achieving this consistency simple since the bulk of the ·OH is produced within 2 ms (Figures 1C, 1D and 4A). To briefly summarize the protocol described in Methods and Materials, the biological reactants

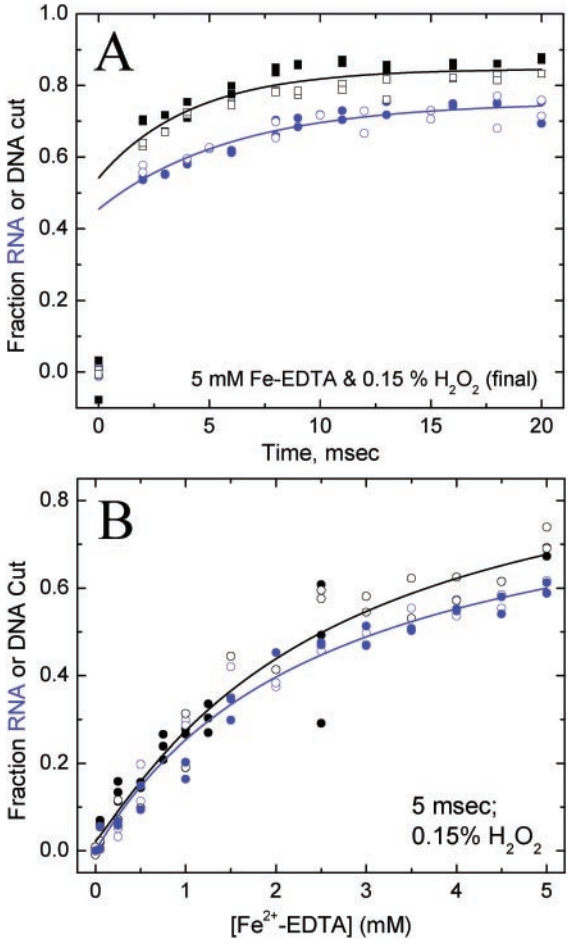

Figure 4. (**A**) Dose–response determinations of the ·OH cleavage of DNA (black) and RNA (blue) following exposure of the nucleic acids to 5 mM Fe(II)-EDTA and 44 mM H_2O_2 for the indicated period of time. The data are best-fit by single exponentials with amplitudes and half-times of $A_{burst} = 0.54$ & 0.44, $A_1 = 0.31 \pm 0.02$ & 0.30 ± 0.02 and $t_1 = 4.2 \pm 0.9$ and 6.1 ± 1.1 ms for DNA and RNA, respectively. The DNA dose–response curve was determined by quantification of the autoradiogram shown in Figure 3B. (**B**) The extent of ·OH mediated cleavage of DNA (black) and RNA (blue) determined at 44 mM H_2O_2 with a 5 ms reaction time as a function of Fe(II)-EDTA concentration. The solid lines are fits of the data to a simple saturation function. Open and closed symbols are replicate experiments in both (A) and (B).

are mixed and the solution allowed to age (Figure 5A; 'A' and 'B'). At a defined time, Fe(II)-EDTA is added to the reactant solution that also contains H_2O_2 to initiate the Fenton reaction; the Fenton reaction proceeds for a constant time and is quenched by the addition of an excess of radical scavenger.

The Mg^{2+}-mediated folding of the *Tetrahymena* ribozyme was followed as a test of the accuracy and precision of fast Fenton footprinting. These experiments were conducted with Fe(II)-EDTA and H_2O_2 concentrations of 0.53 and 80 mM, respectively, determined from a dose-response relationship such as shown in Figure 4B. The time-evolution of changes in ·OH reactivity is clearly seen in a representative autoradiogram (Figure 5B). Quantification of these local measures yields an ensemble of kinetics progress curves that report the changes in local solvent accessibility for each tertiary

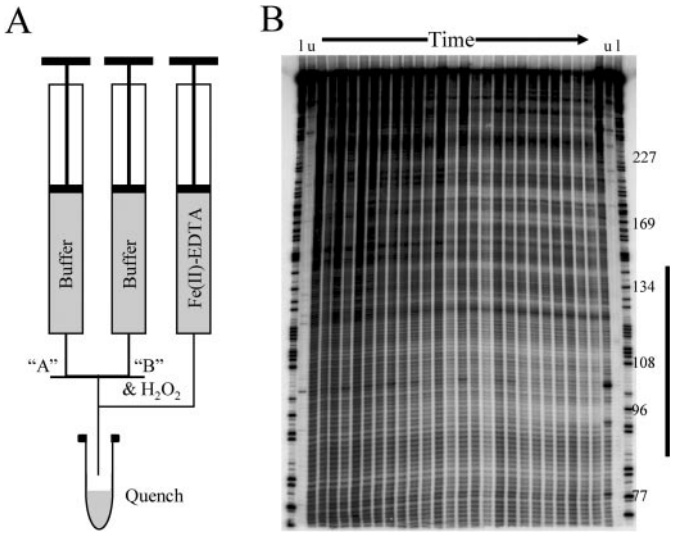

Figure 5. (**A**)Schematic representation of an RNA-folding experiment conducted in the quench-flow mixer. In the experiments shown, 'A' is the ^{32}P-RNA in buffer and 'B' is 20 mM $MgCl_2$ in buffer. The initial concentrations of Fe(II)-EDTA and peroxide are 1.6 mM and 0.81% that yield reagent concentrations after mixing of 0.53 and 80 mM (0.27 %), respectively. Samples of 15 µl were mixed; (**B**) Autoradiogram of a *Tetrahymena* ribozyme Mg^{2+}-mediated folding kinetics experiment conducted in low-salt buffer at 42°C as described in Materials and Methods. The lanes denoted 'l' are the T1 digest ladders while 'u' denotes RNA unexposed to ·OH. The numbers along the side denote the nucleotide numbers. The solid bar along the right of the autoradiogram denotes the nucleotides whose density was quantified with single nucleotide resolution in Figure 2 for the Mg^{2+} folded ribozyme.

contact that defines the folded RNA. Previous studies by synchrotron footprinting studies of the Mg^{2+}-mediated folding reaction initiated from a very low salt initial condition was characterized by a clear hierarchy of P4–P6 domain > periphery > catalytic core with rates of roughly 1.0, 0.1 and 0.02 s^{-1} for the three structural groups (26). Identical results are obtained with the fast Fenton footprinting method (Figures 5B and 6A; orange, magenta and yellow symbols, respectively). A similar comparison was conducted at a high salt initial condition where some synchrotron footprinting progress curves display significant burst amplitudes (Figure 6B and C, red symbols) (42). Sampling of the RNA folding reaction between 5 and 20 ms with fast Fenton footprinting allows the previously hidden kinetics phase to be visualized and a rate constant of ~70 s^{-1} to be assigned to it (Figure 6B and C, closed symbols). The accuracy and precision of the progress curves obtained by the two techniques are comparable.

DISCUSSION

Hydroxyl radical footprinting has achieved prominence by its reporting the solvent accessible surface of macromolecules in solution with as fine as single residue resolution (4). Quantitative studies conducted as a function of either a thermodynamic variable or time provides an ensemble of local measures that track the evolution of solvent accessibility changes (2,5). This collection of measures can then be used to develop and test models of the transition that are connected to the structure of the macromolecule (38,39,43). While the

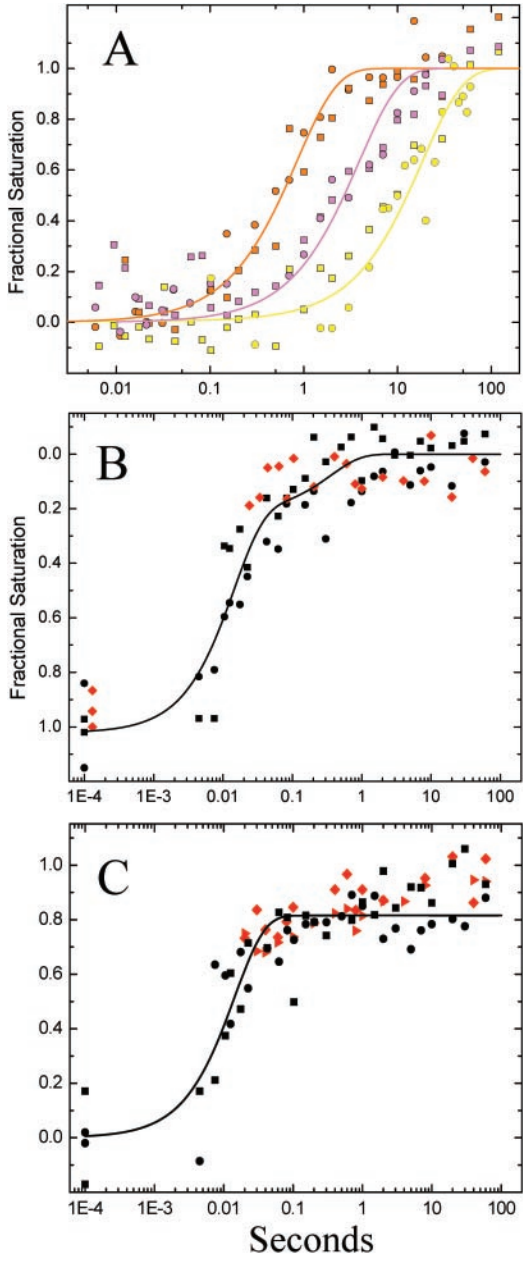

Figure 6. (**A**) Mg^{2+}-mediated kinetics progress curve obtained under the low-salt initial condition by fast Fenton footprinting; the ·OH protections shown are nt 109–112 (orange), 95–97 (magenta) and 278–281 (yellow) representing the P4–P6 domain, peripheral helices and catalytic core protections, respectively. The initial concentrations of Fe(II)-EDTA and peroxide are 1.6 mM and 0.81% that yield reagent concentrations after mixing of 0.53 and 80 mM (0.27%), respectively. The best-fits are to a single exponential decay with rates of 1.19 ± 0.13, 0.21 ± 0.03 and 0.070 ± 0.009 s^{-1}, respectively; (**B**) Mg^{2+}-mediated kinetics progress curve obtained under the high-salt initial condition for nt 122 located in the 'hinge' linking P5abc with P4-P5-P6 by fast Fenton (•) and synchrotron (•) footprinting. The ·OH reactivity of this nucleotide increases during Mg^{2+}-mediated folding resulting in inversion of the fractional saturation. The solid line depicts the best-fit values to a double exponential decay with $k_1 = 70.7$ (−13.0, +25.1) s^{-1}, $k_2 = 2.8$ (−1.8, +6.0) s^{-1}, $A_1 = 0.81 \pm 0.08$ and $A_2 = 0.21 \pm 0.14$; (**C**) Mg^{2+}-mediated kinetics progress curve obtained under the high-salt initial condition for nt 139–140 located within the P4–P6 domain by fast Fenton (•) and synchrotron (43) (•) footprinting. The solid line depicts the best-fit of the fast Fenton data to a single exponential with $k_1 = 69.8 \pm 0.9$ s^{-1}. The squares and circles represent independent experiments. The data points shown at ~ IE-4 in panels B and C represent the Mg^{2+}-free RNA.

development of fast Fenton footprinting is illustrated by the RNA folding kinetics shown in Figure 6, it is immediately applicable to studies of DNA and protein folding as well as protein–protein, protein–DNA and protein–RNA interactions (1,2,4,5). A three-syringe quench-flow mixer and small quantities of inexpensive and readily available chemicals are all that are required to investigate a compelling problem.

The fast footprinting method takes advantage of the efficiency of the Fenton reaction and the amount of and rapidity with which ·OH is generated. The reagent concentrations produce a large burst of ·OH in less than a millisecond (Figure 1C and D) that allow the time resolution of the technique to be pushed to the mixing limit of the apparatus (Figure 6B and C). Under the conditions of our protocol, Fe(II)-EDTA is rapidly oxidized to Fe(III)-EDTA as ·OH is concomitantly produced (Figure 1D) (33) in a stoichiometric reaction (reaction 1). Fe(II) is not reductively recycled by ascorbate (44) or reduced oxygen species (25) to any measurable extent. The large burst of dye or oxidative nucleic acid cleavage at the initiation of the footprinting reaction (Figure 1C) is consistent with the generally accepted rate for Equation 1 of 70 M^{-1} s^{-1} (45).

The close correspondence of the quench-flow and stopped-flow dose–response curves shows that the Fenton reaction is quickly and completely quenched by the addition of an excess of scavenger (Figure 1B and C). Although 5 ms is allowed for ·OH production in our mixing protocol, the majority of the ·OH production occurs within 1 ms (Figure 1C). Thus, even in this simple mixing protocol, data are reliably acquired at times $\geqslant$5 ms (Figure 5B). The improvement in time-resolution relative to synchrotron footprinting was particularly valuable for the analysis of the 'high salt' RNA folding reaction; a previously hidden rapid transition of $\sim$70 s^{-1} is now clearly discernable.

The chemical potential in peroxide that is released in the Fenton reaction can be utilized to overcome less than optimal experimental conditions. Where ·OH scavengers such as Tris, DTT and glycerol must be present in support of the biological reaction being studied, time resolution can be maintained by increasing the concentrations of Fe(II)-EDTA and H_2O_2 (Figure 4B). Studies are in progress to define the technique's limits and develop reference tables for commonly used buffer components. Improvements are also possible with regard to the chelator (33) and metal ion used in the reaction (24).

The protocol presented in this paper is designed to take advantage of the three-syringe quench-flow mixers distributed among laboratories worldwide. However, some biological materials may be adverse to an intimate association with H_2O_2 or Fe(II)-EDTA for periods longer than the several msec duration of the Fenton reaction. This problem can be avoided by the addition of a fourth syringe to the mixing devices that would allow the H_2O_2 and Fe(II)-EDTA to be simultaneously mixed with the aged reactants at the initiation of the Fenton footprinting reaction. Alternatively, additional syringes might be used for more complicated mixing protocols; the ability to conduct time-resolved ·OH footprinting studies with millisecond resolution on the laboratory bench opens the door to the investigation of a myriad array of systems and phenomena.

Time-resolved footprinting is most effectively applied to systems in which the initial, final or both structures are known. In such cases, the collection of local solvent accessibility measures can 'connect the dots' between the initial and final states and thus define the pathway(s) of the transition and provide structural constraints for the intermediate species that are populated along the way. While much can be learned by inspecting collections of footprinting curves, their full potential can only be unlocked through the development of quantitative kinetic models (39,43). Rigorous testing of these models will require the analysis of multiple perturbations of the system under study through mutation, directed mutagenesis and/or analysis of altered reaction conditions. Fast Fenton footprinting will facilitate rigorous model testing by significantly expediting the acquisition of the comprehensive data sets needed to accomplish this important goal.

ACKNOWLEDGEMENTS

We thank Elizabeth Jamison for assistance conducting the experiments with DNA, Lois Polack, Rick Russell and Dan Herschlag for critically reading the manuscript and Donald Crothers, Shar-Yin Huang, Syun-Ru Yeh and Tsuyoshi Egawa for assistance in conducting stopped-flow studies. This work was supported by National Institutes of Health grants PO1–GM066275 and RO1-GM39929 from the Institute of General Medical Sciences. The acquisition of the synchrotron footprinting data shown in Figures 2 and 6 was supported by grant P41-EB0001979 from the Institute of Biomedical Imaging and Bioengineering of the National Institutes of Health. R.H.B. acknowledges financial support from Fordham University and the Research Corporation Cottrell College Science grant CC5650. Funding to pay the Open Access publication charges for this article was provided by The National Institutes of Health.

Conflict of interest statement. None declared.

REFERENCES

1. Petri,V. and Brenowitz,M. (1997) Quantitative nucleic acids footprinting: thermodynamic and kinetic approaches. *Curr. Opin. Biotechnol.*, **8**, 36–44.
2. Brenowitz,M., Chance,M.R., Dhavan,G. and Takamoto,K. (2002) Probing the structural dynamics of nucleic acids by quantitative time-resolved and equilibrium hydroxyl radical 'footprinting'. *Curr. Opin. Struct. Biol.*, **12**, 648–653.
3. Buxton,G.V., Greenstock,C.L., Helman,W.P. and Ross,A.B. (1988) Critical review of rate constants for reactions of hydrated electrons, hydrogen atoms and hydroxyl radicals in aqueous solution. *J. Phys. Chem. Ref. Data.*, **17**, 513–886.
4. Tullius,T.D. and Greenbaum,J.A. (2005) Mapping nucleic acid structure by hydroxyl radical cleavage. *Curr. Opin. Chem. Biol.*, **9**, 127–134.
5. Guan,J.Q. and Chance,M.R. (2005) Structural proteomics of macromolecular assemblies using oxidative footprinting and mass spectrometry. *Trends Biochem. Sci.*, **30**, 583–592.
6. Tullius,T.D. and Dombroski,B.A. (1986) Hydroxyl radical 'footprinting': high-resolution information about DNA- protein contacts and application to lambda repressor and Cro protein. *Proc. Natl Acad. Sci. USA*, **83**, 5469–5473.
7. Tullius,T.D. and Dombroski,B.A. (1985) Iron(II) EDTA used to measure the helical twist along any DNA molecule. *Science*, **230**, 679–681.
8. King,P.A., Anderson,V.E., Edwards,J.O., Gustafson,G., Plumb,R.C. and Suggs,J.W. (1992) A stable solid that generates hydroxyl radical upon dissolution in aqueous solution. Reaction with proteins and nucleic acid. *J. Am. Chem. Soc.*, **114**, 5430–5432.

9. King,P.A., Jamison,E., Strahs,D., Anderson,V.E. and Brenowitz,M. (1993) 'Footprinting' proteins on DNA with peroxonitrous acid. *Nucleic Acids Res*., **21**, 2473–2478.
10. Chaulk,S.G. and MacMillan,A.M. (2000) Characterization of the *Tetrahymena* ribozyme folding pathway using the kinetic footprinting reagent peroxynitrous acid. *Biochemistry*, **39**, 2–8.
11. Sharp,J.S., Becker,J.M. and Hettich,R.L. (2004) Analysis of protein solvent accessible surfaces by photochemical oxidation and mass spectrometry. *Anal. Chem*., **76**, 672–683.
12. Aye,T.T., Low,T.Y. and Sze,S.K. (2005) Nanosecond laser-induced photochemical oxidation method for protein surface mapping with mass spectrometry. *Anal. Chem*., **77**, 5814–5822.
13. Hambly,D.M. and Gross,M.L. (2005) Laser flash photolysis of hydrogen peroxide to oxidize protein solvent-accessible residues on the microsecond timescale. *J. Am. Soc. Mass Spectrom*., **16**, 2057–2063.
14. Maleknia,S.D., Brenowitz,M. and Chance,M.R. (1999) Millisecond radiolytic modification of peptides by synchrotron X-rays identified by mass spectrometry. *Anal. Chem*., **71**, 3965–3973.
15. Hayes,J.J., Kam,L. and Tullius,T.D. (1990) Footprinting protein–DNA complexes with gamma-rays. *Methods Enzymol*., **186**, 545–549.
16. Ottinger,L.M. and Tullius,T.D. (2000) High-resolution *in vivo* footprinting of a protein–DNA complex using gamma radiation. *J. Am. Chem. Soc*., **122**, 5901–5902.
17. Sclavi,B., Woodson,S., Sullivan,M., Chance,M.R. and Brenowitz,M. (1997) Time-resolved synchrotron X-ray 'footprinting', a new approach to the study of nucleic acid structure and function: application to protein- DNA interactions and RNA folding. *J. Mol. Biol*., **266**, 144–159.
18. Fenton,H.J.H. (1894) What species is responsible for strands scission in the reaction of $[FeIIEDTA]^{2-}$ with H_2O_2 with DNA? *J. Chem. Soc*., **6**, 899.
19. Haber,F. and Weiss,J. (1934) The catalytic decomposition of hydrogen peroxide by iron salts. *Proc. R Soc. Lond. A*, **147**, 332–351.
20. Pogozelski,W.K., McNeese,T.J. and Tullius,T.D. (1995) What Species is Responsible for Strand Scission in the reaction of [FeIIEDTA]2- with H2O2 with DNA? *J. Am. Chem. Soc*., **117**, 11673–11679.
21. Tullius,T.D., Dombroski,B.A., Churchill,M.E. and Kam,L. (1987) Hydroxyl radical footprinting: a high-resolution method for mapping protein-DNA contacts. *Methods Enzymol*., **155**, 537–558.
22. Dixon,W.J., Hayes,J.J., Levin,J.R., Weidner,M.F., Dombroski,B.A. and Tullius,T.D. (1991) Hydroxyl radical footprinting. *Methods Enzymol*., **208**, 380–413.
23. Hampel,K.J. and Burke,J.M. (2001) Time-resolved hydroxyl-radical footprinting of RNA using Fe(II)-EDTA. *Methods*, **23**, 233–239.
24. Goldstein,S. and Meyerstein,D. (1999) Comments on the mechanism of the 'Fenton-Like' reaction. *Acc. Chem. Res*., **32**, 547–550.
25. Yoon,J., Lee,Y. and Kim,S. (2001) Investigation of the reaction pathway of OH radicals produced by Fenton oxidation in the conditions of wastewater treatment. *Water Sci. Technol*., **44**, 15–21.
26. Sclavi,B., Sullivan,M., Chance,M.R., Brenowitz,M. and Woodson,S.A. (1998) RNA folding at millisecond intervals by synchrotron hydroxyl radical footprinting. *Science*, **279**, 1940–1943.
27. Ralston,C.Y., Sclavi,B., Sullivan,M., Deras,M.L., Woodson,S.A., Chance,M.R. and Brenowitz,M. (2000) Time-resolved synchrotron X-ray footprinting and its application to RNA folding. *Methods Enzymol*., **317**, 353–368.
28. Zaug,A.J., Grosshans,C.A. and Cech,T.R. (1988) Sequence-specific endoribonuclease activity of the *Tetrahymena* ribozyme: enhanced cleavage of certain oligonucleotide substrates that form mismatched ribozyme–substrate complexes. *Biochemistry*, **27**, 8924–8931.
29. Patikoglou,G.A., Kim,J.L., Sun,L., Yang,S.H., Kodadek,T. and Burley,S.K. (1999) TATA element recognition by the TATA box-binding protein has been conserved throughout evolution. *Genes Dev*., **13**, 3217–3230.
30. Petri,V., Hsieh,M., Jamison,E. and Brenowitz,M. (1998) DNA sequence-specific recognition by the Saccharomyces cerevisiae 'TATA' binding protein: promoter-dependent differences in the thermodynamics and kinetics of binding. *Biochemistry*, **37**, 15842–15849.
31. Ou,B., Hampsch-Woodill,M., Flanagan,J., Deemer,E.K., Prior,R.L. and Huang,D. (2002) Novel fluorometric assay for hydroxyl radical prevention capacity using fluorescein as the probe. *J. Agri. Food Chem*., **50**, 2772–2777.
32. Chen,F., Ma,W., He,J. and Zhao,J. (2002) Fenton degradation of malachite green catalyzed by aromatic additives. *J. Phys. Chem*., **106**, 9485–9490.
33. Rush,J.D. and Koppenol,W.H. (1987) The reaction between ferrous polyaminocarboxylate complexes and hydrogen peroxide: an investigation of the reaction intermediates by stopped flow spectrophotometry. *J. Inorg. Biochem*., **29**, 199–215.
34. Hsieh,M. and Brenowitz,M. (1996) Quantitative kinetics footprinting of protein–DNA association reactions. *Methods Enzymol*., **274**, 478–492.
35. Sclavi,B., Woodson,S., Sullivan,M., Chance,M. and Brenowitz,M. (1998) Following the folding of RNA with time-resolved synchrotron X-ray footprinting. *Methods Enzymol*., **295**, 379–402.
36. Brenowitz,M., Senear,D.F., Shea,M.A. and Ackers,G.K. (1986) Quantitative DNase footprint titration: a method for studying protein–DNA interactions. *Methods Enzymol*., **130**, 132–181.
37. Das,R., Laederach,A., Perlman,S.M., Herschlag,D. and Altman,R.B. (2005) SAFA: Semi-Automated Footprinting Analysis software for high-throughput quantification of nucleic acid footprinting experiments. *RNA*, **11**, 344–354.
38. Dhavan,G.M., Crothers,D.M., Chance,M.R. and Brenowitz,M. (2002) Concerted binding and bending of DNA by *Escherichia coli* integration host factor. *J. Mol. Biol*., **315**, 1027–1037.
39. Laederach,A.L., Shcherbakova,I., Liang,M.P., Brenowitz,M. and Altman,R.B. (2006) Reconstructing RNA folding pathways from local probes of macromolecular structure. *J. Mol. Biol.* in press.
40. Pastor,N., Weinstein,H., Jamison,E. and Brenowitz,M. (2000) A detailed interpretation of OH radical footprints in a TBP–DNA complex reveals the role of dynamics in the mechanism of sequence-specific binding. *J. Mol. Biol*., **304**, 55–68.
41. Cate,J.H., Gooding,A.R., Podell,E., Zhou,K., Golden,B.L., Kundrot,C.E., Cech,T.R. and Doudna,J.A. (1996) Crystal structure of a group I ribozyme domain: principles of RNA packing [see comments]. *Science*, **273**, 1678–1685.
42. Thorp,H.H. (2000) The importance of being r: greater oxidative stability of RNA compared with DNA. *Chem. Biol*., **7**, R33–36.
43. Uchida,T., Takamoto,K., He,Q., Chance,M.R. and Brenowitz,M. (2003) Multiple monovalent ion-dependent pathways for the folding of the L-21 *Tetrahymena thermophila* ribozyme. *J. Mol. Biol*., **328**, 463–478.
44. Sclavi,B., Zaychikov,E., Rogozina,A., Walther,F., Buckle,M. and Heumann,H. (2005) Real time characterization of intermediates in the pathway to open complex formation by *E. coli* RNA polymerase at the T7A1 promoter. *Proc. Natl Acad. Sci. USA*, **102**, 4706–4711.
45. Udenfriend,S., Clark,C.T., Axelrod,J. and Brodie,B.B. (1954) Ascorbic acid in aromatic hydroxylation. I. A model system for aromatic hydroxylation. *J. Biol. Chem*., **208**, 731–739.
46. Walling,C. (1975) Fenton's reagent revisited. *Acc. Chem. Res*., 8.

APPENDIX: SETUP OF KINTEK RQF-3 STEPPER MOTOR CONTROL PROGRAM

In footprinting experiments, reagents A and B are mixed to initiate the reaction being studied. After a defined aging time, the ·OH footprinting reaction is initiated by the addition of Fe(II)-EDTA from the 'quench' syringe. The ·OH footprinting reaction takes place in the exit tube of the KinTek® mixer until the expulsion of the sample into the collection tube, indicated by the red box in Figure A1. The duration of this reaction is proportional to the flow rate of, and distance traveled by, the solution containing both Fe(II)-EDTA and H_2O_2. While either flow rate or distance can be modified to control the reaction time, we chose to do a little of both. We trimmed the exit tube of the KinTek® mixer to ~5 cm. We also increased the minimal motor speed so that 5 ms is allotted for the ·OH footprinting reaction.

The volume of the exit tube was calibrated following the manufacturer's protocol. The motor speed necessary to

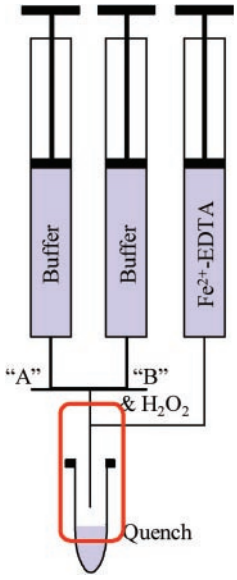

Figure A1. A schematic representation of quench-flow footprinting folding or binding experiment. The red box indicates the exit loop, where the Fenton mediated cleavage reaction occurs. Changes in the reaction time can be achieved by alteration of either the length of the exit tube, the flow rate through it or both parameters.

achieve a required ·OH footprinting reaction time was calculated by

$$\text{speed}_{\text{RPM}} = \frac{\text{volume}_{\text{exit-tube}} \times 60}{1.5 \times \text{volume}_{\text{revolution}} \times \text{time}_{\text{reaction}}}$$

Each of the parameters is defined in the RQF-3 user manual. Parameter FLT11 should be changed in line 8 of manufacturer's control program QF3B.PAC so that desired value of $\text{speed}_{\text{RPM}} = 1.2 \times \text{FLT11}$. This default parameter ensures the motor speed to be equal to the calculated $\text{speed}_{\text{RPM}}$ for the times longer than maximal time for loop 7 (from 'Change parameters' option) and will only vary within reasonable limits for the shorter times. For example, for the experiments shown in Figures 4 and 5 the volume of the exit tube is 54 µl and FLT11 = 430. These parameters yield a ·OH reaction time of 5 ms for the long aging times (loop 7). The ·OH reaction time ranges from 3 to 6 ms for the aging times up to 36 ms that are achieved using loops 1–6.

The file QF3B.PAC can be edited using a text editor such as Microsoft's WordPad. When the new value for parameter FLT11 calculated as described above is entered, the program should be saved and uploaded into the controller. Uploading modified control code requires software provided by the manufacturer.